

Progress towards an improved particle flow algorithm at CMS with machine learning

Farouk Mokhtar¹, Joosep Pata², Javier Duarte¹, Eric Wulff³,
Maurizio Pierini³ and Jean-Roch Vlimant⁴

(on behalf of the CMS Collaboration)

¹University of California San Diego, La Jolla, CA 92093, USA

²NICPB, Rävåla pst 10, 10143 Tallinn, Estonia

³European Organization for Nuclear Research (CERN), CH 1211, Geneva 23, Switzerland

⁴California Institute of Technology, Pasadena, CA 91125, USA

E-mail: fmokhtar@ucsd.edu, joosep.pata@cern.ch, jduarte@ucsd.edu

Abstract. The particle-flow (PF) algorithm, which infers particles based on tracks and calorimeter clusters, is of central importance to event reconstruction in the CMS experiment at the CERN LHC, and has been a focus of development in light of planned Phase-2 running conditions with an increased pileup and detector granularity. In recent years, the machine-learned particle-flow (MLPF) algorithm, a graph neural network that performs PF reconstruction, has been explored in CMS, with the possible advantages of directly optimizing for the physical quantities of interest, being highly reconfigurable to new conditions, and being a natural fit for deployment to heterogeneous accelerators. We discuss progress in CMS towards an improved implementation of the MLPF reconstruction, now optimized using generator/simulation-level particle information as the target for the first time. This paves the way to potentially improving the detector response in terms of physical quantities of interest. We describe the simulation-based training target, progress and studies on event-based loss terms, details on the model hyperparameter tuning, as well as physics validation with respect to the current PF algorithm in terms of high-level physical quantities such as the jet and missing transverse momentum resolutions. We find that the MLPF algorithm, trained on a generator/simulator level particle information for the first time, results in broadly compatible particle and jet reconstruction performance with the baseline PF, setting the stage for improving the physics performance by additional training statistics and model tuning.

1. Introduction

Particle-flow (PF) reconstruction is a global event reconstruction that combines information from different subdetectors in CMS (e.g. the tracker and the electromagnetic and hadronic calorimeters) to reconstruct stable particles [1]. The machine-learned particle-flow (MLPF) algorithm is a graph neural network (GNN) trained to perform PF reconstruction via supervised machine learning (ML) [2, 3, 4]. As with the baseline rule-based PF, the inputs to MLPF are tracks and calorimeter clusters (see Figure 1), and the outputs are stable PF candidate particles. The advantages of MLPF include the possibility of deployment on heterogeneous computing accelerators (e.g. GPUs) and reoptimizing the algorithm in light of new experimental conditions.

In this work, we summarize the latest developments of MLPF in CMS, which includes the

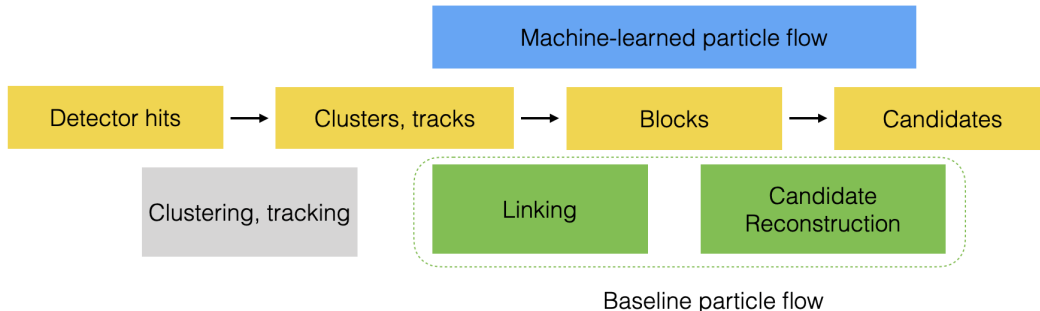


Figure 1. A schematic overview of MLPF in the proposed reconstruction scheme.

development of a new generator/simulation-level training target, without referencing an existing PF algorithm. It should be noted that this effort fits in the wider context of implementing reconstruction algorithms for current and future detectors, partly or fully using trainable, differentiable ML [5, 6, 7, 8, 9]. Results from our experiments show that we can achieve results that are largely compatible, and in some cases better, than standard PF. The full set of results is available in the accompanying Detector Performance note [10].

2. Particle-level training target definition

The MLPF training target is based on detector simulation information to closely approximate the input the simulation receives from the generator. The truth particles for MLPF are the root nodes of the GEANT4 simulation tree, consisting of simulated particle decays and interactions with matter, defined via the following truth definition algorithm.

The truth algorithm takes as input the tree of GEANT4 simulation particles, searches for the earliest particles whose children leave detectable hits in either the tracker or calorimeters¹. Given these decay tree root particles, we first address double-counting by removing the particles that have overlapping GEANT4 simulation track identifiers.

Now knowing the set of root simulation particles whose decay products in principle interact with the detector, we have to define which of those we wish to reconstruct as PF particles, and with which granularity. The simulation particles are cleaned as follows:

- (i) Coalesce particle labels according to PF granularity: any charged hadrons are assigned to a single charged hadron class, all neutral hadrons are assigned to a single neutral hadron class, etc.
- (ii) Geometrically overlapping particles that leave energy deposits only to the same calorimeter cluster are not reconstructable separately, and are thus merged, keeping the label of the highest-energy particle.
- (iii) Electrons or muons with $p_T < 1$ GeV are relabeled as charged or neutral hadrons, based on the deposited track and calorimeter energy, to approximate the behaviour of the baseline PF algorithm.
- (iv) to mimic the response of baseline PF, particles outside the tracker acceptance are labeled as HF hadronic or HF electromagnetic, depending on the energy deposits to the respective calorimeters

The resulting set of simulated particles is denoted as the MLPF ground truth. Comparisons between PF and the MLPF truth are available in pages 5–7 of the Detector Performance note [10].

¹ We use the CMSSW `CaloParticle` and `TrackingParticle` modules to traverse the simulation tree

3. Datasets

With the algorithm above, we generate datasets for MLPF truth validation and subsequent model optimization. We use the official CMS software² for sample generation, simulation and baseline PF reconstruction, with the center of mass energy $\sqrt{s} = 14$ TeV and running conditions corresponding to Run 3. For the samples with pileup, we use a flat pileup (PU) profile with a Poisson distribution in the range 55–75, mixed in from a high-statistics minimum bias dataset³. The training and validation is carried out on a mixture of all the samples listed in Table 1.

physics process	PU configuration	MC events
top quark-antiquark pairs ($t\bar{t}$)	flat 55–75	100 k
QCD $\hat{p}_T \in [15, 3000]$ GeV	flat 55–75	100 k
QCD $\hat{p}_T \in [3000, 7000]$ GeV	flat 55–75	100 k
Z $\rightarrow \tau\tau$ all-hadronic	flat 55–75	100 k
single e flat $p_T \in [1, 1000]$ GeV	no PU	10 k
single μ log-flat $p_T \in [0.1, 2000]$ GeV	no PU	10 k
single π^0 flat $p_T \in [0, 1000]$ GeV	no PU	10 k
single π^\pm flat $p_T \in [0.7, 1000]$ GeV	no PU	10 k
single τ flat $p_T \in [1, 1000]$ GeV	no PU	10 k
single γ flat $p_T \in [1, 1000]$ GeV	no PU	10 k
single p flat $p_T \in [0.7, 1000]$ GeV	no PU	10 k
single n flat $p_T \in [0.7, 1000]$ GeV	no PU	10 k

Table 1. MC simulation samples used for optimizing the MLPF model. The kinematic quantity \hat{p}_T is computed as the scalar sum of the outgoing generator-level partons.

4. Event loss scans

Since the end goal of PF is global event reconstruction, we expect that MLPF, in addition to reconstructing PF-candidates, is able to reconstruct event-level quantities with high accuracy, such as those related to jets and the missing transverse momentum. For each event, jets are clustered from reconstructed or generator-level particles using the anti- k_T algorithm [11, 12] with a distance parameter of 0.4 (AK4 jets). The missing transverse momentum vector \vec{p}_T^{miss} is computed as the negative vector sum of the transverse momenta of all the PF candidates in an event, and its magnitude is denoted as p_T^{miss} [13]. The pileup per particle identification (PUPPI) algorithm [14, 15] is applied to reduce the pileup dependence of the jet and \vec{p}_T^{miss} observables [13].

While the basic MLPF algorithm incorporates a per-particle loss, it is interesting to study if including additional terms in the loss function can lead to better event-level reconstruction. In general, the simple approach of clustering the reconstructed particles to jets, and comparing the resulting reconstructed jets to the generator-level jets is not practical, as fast, differentiable and GPU-optimized jet clustering algorithms are not yet available. We have tested the following proxy event-level loss terms:

- (i) Baseline: only the basic MLPF per-particle classification and regression loss
- (ii) Sliced Wasserstein distance: compute a p_T -weighted mass transportation cost in the $[\eta, \sin \phi, \cos \phi]$ space between the set of reconstructed and target particles, approximating the metric through random projections (slicing)
- (iii) Generator-level jet log cosh: assuming that the reconstructed particles are clustered to the

² CMSSW_12_3_0_pre6

³ /RelValMinBias_14TeV/CMSSW_12_2_0_pre2-122X_mcRun3_2021_realistic_v1_HighStat-v1/GEN-SIM

same jets as the target (MLPF truth) particles, compute the effective reconstructed jet p_T values, and compare these to the generator-level jet p_T values using a log cosh loss

- (iv) Missing transverse momentum: compute the reconstructed p_T^{miss} from the reconstructed particle candidates, and compare it with a mean squared error loss term with the target p_T^{miss}

Comparisons are shown in Figure 2. We monitor the median and interquartile range of the jet response distribution, defined such that the optimal values for both are zero. We find that none of the tested loss functions improve the jet-level physics quantities that we observe during the training process, with the baseline, i.e. no additional event loss term added to the particle-level loss, performing the best.

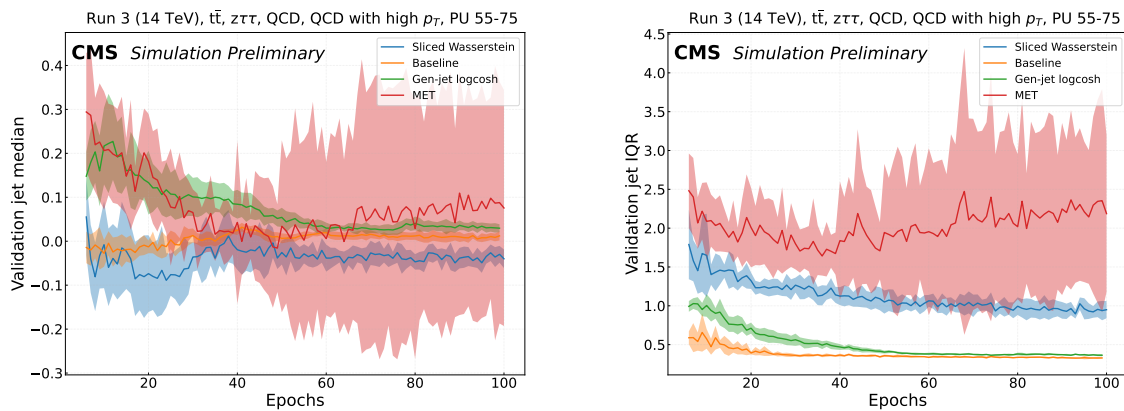


Figure 2. Comparison of the jet response median (left) and interquartile range (right) using different event-level loss terms. Solid lines show the mean of 10 trainings with identical configurations and shaded regions show the mean plus and minus one standard deviation of the 10 trainings.

5. Event-level validation in CMSSW

The MLPF algorithm is integrated with CMS software framework (CMSSW) through an optional (default disabled) switch, using ONNXRUNTIME for inference. The purpose of this validation is to test MLPF in a real integration, completely independently of the ML training data format and software framework. We demonstrate the results of enabling MLPF in CMSSW reconstruction instead of standard PF by validating on the following samples, which were not used in training: QCD multijet⁴ with $\hat{p}_T \in [15, 3000]$ GeV (46 k events)⁵ and top quark-antiquark pairs, or $t\bar{t}$, (8 k events)⁶.

The following results are event-level validation extracted directly from the MINIAOD event data. We also test the performance of MLPF on the particle-level quantities, which are presented in full in the Detector Performance note [10].

⁴ The background from standard model events composed uniquely of jets produced through the strong interaction is referred to as quantum chromodynamics (QCD) multijet events.

⁵ /RelValQCD_FlatPt_15_3000HS_14/CMSSW_12_3_0_pre6-PU_123X_mcRun3_2021_realistic_v11-v1/GEN-SIM-DIGI-RAW

⁶ /RelValTTbar_14TeV/CMSSW_12_3_0_pre6-PU_123X_mcRun3_2021_realistic_v11-v1/GEN-SIM-DIGI-RAW

5.1. Jets

The comparison of generator-level and reconstructed jet distributions from PF and MLPF is shown on Figure 3. The jet distributions between PF and MLPF are broadly compatible, highlighting the jet reconstruction performance of the purely ML-based MLPF reconstruction that was trained on a generator/simulator particle level target.

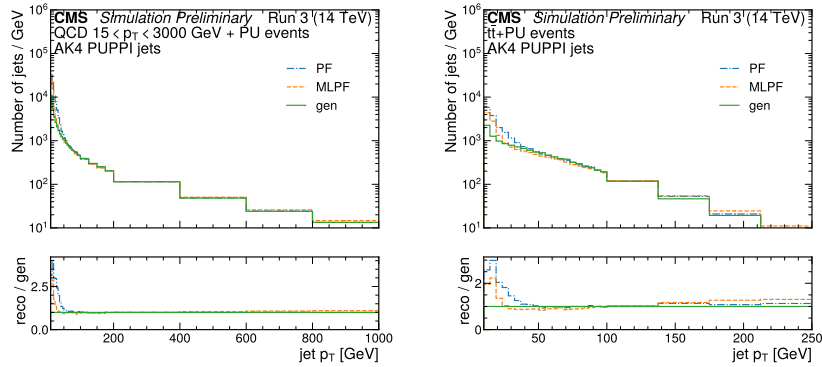


Figure 3. Reconstructed PUPPI jet p_T distributions with PF and MLPF, compared with the true generator-level jet distribution in QCD (left) and $t\bar{t}$ (right) samples with pileup, reconstructed in CMSSW.

5.2. Missing traverse momentum

The comparison of generator-level p_T^{miss} to reconstructed PUPPI p_T^{miss} distributions from PF and MLPF is shown on Figure 4. For the QCD sample in particular, we observe high- p_T tails in both PF and MLPF, which are more prominent in MLPF. Work is currently ongoing to reduce this effect through improved data samples and additional training.

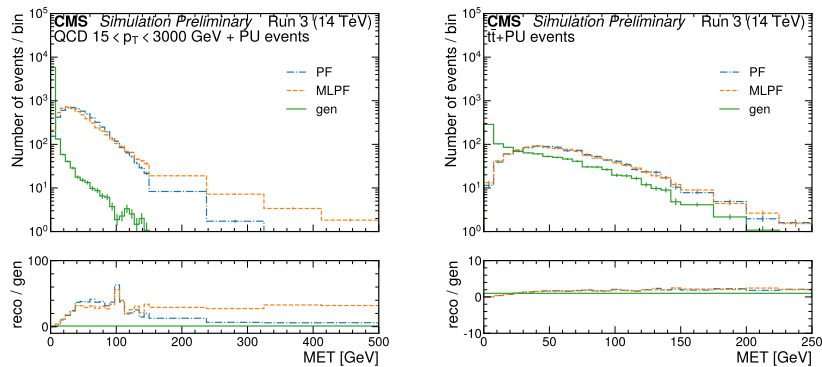


Figure 4. Reconstructed PUPPI p_T^{miss} distributions with PF and MLPF, compared with the true generator-level p_T^{miss} distribution in QCD (left) and $t\bar{t}$ (right) samples with pileup, reconstructed in CMSSW.

6. Conclusion

We have defined a new generator/simulator-level machine-learned particle-flow (MLPF) training target which enables the MLPF-based reconstruction, in principle, to surpass the baseline PF algorithm reconstruction. We presented comparisons between PF and MLPF on the particle-level, where the MLPF performance is comparable to the rule-based particle-flow (PF). As a particular quantitative improvement, we find that the neutral hadron p_T response width is improved by about a factor of 2, while the MLPF reconstruction is fully efficient at a lower fake rate than the baseline PF for calorimeter clusters with $E > 10$ GeV. We also compare the performance on the event level, directly in CMS software framework (CMSSW), where we find broadly comparable performance for jets, while the p_T^{miss} performance is affected by slightly larger tails in MLPF than in PF which we plan to address in a follow-up. To improve the reconstruction of the event-level quantities further, we have explored the use of additional event-level loss terms, however, we find that in this case, the baseline particle-level loss performs the best.

The next steps include further work on the training datasets and on the machine learning (ML) modelling and optimization, to further improve the reconstruction of complex event-based quantities. It is also worthwhile to explore the application of explainable AI techniques on MLPF, since a common disadvantage of ML-based algorithms is a lack of interpretability. In previous work we have explored such techniques in order to gain insight into the model's decision-making [16]. It is interesting to revisit such studies again, now that we have a well-defined MLPF truth. Additionally, we also plan to rerun our hypertuning on HPC resources in light of the new dataset [17].

7. Acknowledgements

We thank our colleagues in the CMS Collaboration, especially in the Particle Flow, Physics Performance and Dataset, Offline and Computing, and Machine Learning groups, in particular Kenichi Hatakeyama, Lindsey Gray, Jan Kieseler, Danilo Piparo, Gregor Kasieczka, Salvatore Rappoccio, Kaori Maeshima, Kenneth Long, and Juska Pekkanen for helpful feedback in the course of this work. JP was supported by the Mobilitas Plus Grants MOBTP187, PRG780 and MOBTT86 of the Estonian Research Council. JD and FM were supported by DOE Award Nos. DE-SC0021187 and DE-SC0021396 (FAIR4HEP) and NSF Cooperative Agreement OAC-2117997 (A3D3). FM was also supported by a UCSD HDSI fellowship and an IRIS-HEP fellowship through NSF Cooperative Agreement OAC-1836650. EW was supported by the CoE RAISE Project which have received funding from the European Union's Horizon 2020 – Research and Innovation Framework Programme H2020-INFRAEDI-2019-1 under grant agreement no. 951733. Access to GPUs was supported in part by NSF awards CNS-1730158, ACI-1540112, ACI-1541349, OAC-1826967, OAC-2112167, CNS-2100237, CNS-2120019, the University of California Office of the President, and the University of California San Diego's California Institute for Telecommunications and Information Technology/Qualcomm Institute. Thanks to CENIC for the 100 Gbps networks.

References

- [1] CMS Collaboration. “Particle-flow reconstruction and global event description with the CMS detector”. In: *JINST* 12.10 (2017), P10003. DOI: [10.1088/1748-0221/12/10/P10003](https://doi.org/10.1088/1748-0221/12/10/P10003).
- [2] Joosep Pata et al. “MLPF: Efficient machine-learned particle-flow reconstruction using graph neural networks”. In: *Eur. Phys. J. C* 81.5 (2021), p. 381. DOI: [10.1140/epjc/s10052-021-09158-w](https://doi.org/10.1140/epjc/s10052-021-09158-w).
- [3] Joosep Pata et al. “Machine Learning for Particle Flow Reconstruction at CMS”. In: *J. Phys. Conf. Ser.* 2438.1 (2023), p. 012100. DOI: [10.1088/1742-6596/2438/1/012100](https://doi.org/10.1088/1742-6596/2438/1/012100).

- [4] CMS Collaboration. *Machine Learning for Particle Flow Reconstruction at CMS*. CMS Detector Performance Note CMS-DP-2021-030. 2021. URL: <https://cds.cern.ch/record/2792320>.
- [5] Bruno Alves, Felice Pantaleo, and Marco Rovere. “Clustering in the Heterogeneous Reconstruction Chain of the CMS HGCALE Detector”. In: *J. Phys. Conf. Ser.* 2438.1 (2023), p. 012015. DOI: [10.1088/1742-6596/2438/1/012015](https://doi.org/10.1088/1742-6596/2438/1/012015).
- [6] Felice Pantaleo and Marco Rovere. “The Iterative Clustering framework for the CMS HGCALE Reconstruction”. In: *J. Phys. Conf. Ser.* 2438.1 (2023), p. 012096. DOI: [10.1088/1742-6596/2438/1/012096](https://doi.org/10.1088/1742-6596/2438/1/012096).
- [7] Saptaparna Bhattacharya et al. “GNN-based end-to-end reconstruction in the CMS Phase 2 High-Granularity Calorimeter”. In: *J. Phys. Conf. Ser.* 2438.1 (2023), p. 012090. DOI: [10.1088/1742-6596/2438/1/012090](https://doi.org/10.1088/1742-6596/2438/1/012090).
- [8] Francesco Armando Di Bello et al. “Towards a Computer Vision Particle Flow”. In: *Eur. Phys. J. C* 81.2 (2021), p. 107. DOI: [10.1140/epjc/s10052-021-08897-0](https://doi.org/10.1140/epjc/s10052-021-08897-0).
- [9] Francesco Armando Di Bello et al. “Reconstructing particles in jets using set transformer and hypergraph prediction networks”. Dec. 2022.
- [10] CMS Collaboration. *Progress towards an improved particle flow algorithm at CMS with machine learning*. CMS Detector Performance Note CMS-DP-2022-061. 2022. URL: <http://cds.cern.ch/record/2842375>.
- [11] Matteo Cacciari, Gavin P. Salam, and Gregory Soyez. “The anti- k_T jet clustering algorithm”. In: *JHEP* 04 (2008), p. 063. DOI: [10.1088/1126-6708/2008/04/063](https://doi.org/10.1088/1126-6708/2008/04/063).
- [12] Matteo Cacciari, Gavin P. Salam, and Gregory Soyez. “FastJet user manual”. In: *Eur. Phys. J. C* 72 (2012), p. 1896. DOI: [10.1140/epjc/s10052-012-1896-2](https://doi.org/10.1140/epjc/s10052-012-1896-2).
- [13] Albert M Sirunyan et al. “Performance of missing transverse momentum reconstruction in proton-proton collisions at $\sqrt{s} = 13$ TeV using the CMS detector”. In: *JINST* 14 (2019), P07004. DOI: [10.1088/1748-0221/14/07/P07004](https://doi.org/10.1088/1748-0221/14/07/P07004).
- [14] Albert M Sirunyan et al. “Pileup mitigation at CMS in 13 TeV data”. In: *JINST* 15 (2020), P09018. DOI: [10.1088/1748-0221/15/09/p09018](https://doi.org/10.1088/1748-0221/15/09/p09018).
- [15] Daniele Bertolini et al. “Pileup Per Particle Identification”. In: *JHEP* 10 (2014), p. 059. DOI: [10.1007/JHEP10\(2014\)059](https://doi.org/10.1007/JHEP10(2014)059).
- [16] Farouk Mokhtar et al. “Explaining machine-learned particle-flow reconstruction”. In: *4th Machine Learning and the Physical Sciences Workshop at the 35th Conference on Neural Information Processing Systems*. 2021.
- [17] Eric Wulff, Maria Girone, and Joosep Pata. “Hyperparameter optimization of data-driven AI models on HPC systems”. In: *J. Phys. Conf. Ser.* 2438.1 (2023), p. 012092. DOI: [10.1088/1742-6596/2438/1/012092](https://doi.org/10.1088/1742-6596/2438/1/012092).